ISTITUTO NAZIONALE DI FISICA NUCLEARE

Sezione di Roma 2

INFN/TC-96/20
30 Ottobre 1996

L. Cerrito, M. Gatta, M. Imhof, L. Paoluzi, E. Santovetti, S. Weseler:

A SET UP FOR TESTING THE PRIMARY IONIZATION COUNTING IN A DRIFT CHAMBER AT NORMAL CONDITION

PACS: 06.70.Ep

Submitted to Nuclear Instruments & Methods

SIS–Pubblicazioni
dei Laboratori Nazionali di Frascati

INFN – Istituto Nazionale di Fisica Nucelare
Sezione di Roma 2

INFN/TC–96/20
30 Ottobre 1996

A SET UP FOR TESTING THE PRIMARY IONIZATION COUNTING IN A DRIFT CHAMBER AT NORMAL CONDITION

L. Cerrito[1], M. Gatta[1], M. Imhof[2], L. Paoluzi[1], E. Santovetti[1], S. Weseler[2]
[1)] INFN–Sezione di Roma 2 and Physics Department of 2nd University of Rome, Via della Ricerca Scientifica 1, Tor Vergata, I–00133 Roma, Italy
[2)] Institut für Experimentelle Kernphysic, Universität Karlsruhe, D–76021 Germany

ABSTRACT
The feasibility of cluster counting in a realistic drift chamber must be studied in detail. A large size test drift chamber with 147 sqared cells has been built to be operated with Helium based gases. Twenty of the cells are equipped with fast electronics and digitizers to capture the complete waveforms which will be analyzed offline. The system that has been operated succefully in a test beam will be described in detail.

INTRODUCTION
The energy loss of a charged particle in a medium happens in discrete acts of exitation and ionization uniformly distributed along the track. In same cases the energy of these primary electrons is sufficiently high to produce secondary electrons. As these electrons are produced more closely in space than the average distance between primaries, one may speak of cluster of electrons. The distribution of the number of electrons in a cluster has a large variance. The most commonly method used to measure the energy loss (and $\beta\gamma$ of a particle) samples the total charge in small cells and reduces the variance by discarding 30-40% of the highest values. The number of primary ionization (PI) acts (clusters) per unit lenght is a function of $\beta\gamma$, too. A measurement of the number of clusters produced in a large volume drift chamber would be an ideal way to identify particles, because the Poisson distribution of the number of clusters behaves statistically much better than the Landau distribution in the charge integration method, thus providing a better separation.

In 1969 Davidenko et al.[1] pointed out the advantage of counting the primary ionization with respect to the charge integration method and performed some measurement using a streamer chamber at low pressure. The main problem in applying the cluster counting (CC) was the short time distance between electrons at normal condition . Since then, several attempt have been made to measure the PI. Typically streamer chambers with variable time delay [1,2] have been used. In 1979-1980 [3,4] Walenta built and tested a time expansion chamber to spread the clusters in time. With their chamber they obtained interesting results and showed that the major part of the relativistic rise is due to the production of primaries electrons. Breskin[5] did a similar measurement with a fast photomultiplier detecting photons emitted in the avalanche.

Large improvements in electronics integration now allows to use an electronic readout to measure the PI in a drift chamber at normal pressure conditions. The cluster counting method is based on a compromise between cluster density, gas diffusion and time resolution to count the PI acts while discarding the secondary production. Moving from an infinite time resolution to a poor one one passes from a Landau distribution to an inefficent Poisson regime. Helium based gas mixtures have been proposed for drift chambers in new experiments to reduce the multiple scattering contribution to the track parameter resolution. Helium has the additional advantage to have the clusters well separated in space giving a sufficiently large separation in arrival time at the sense wire to be detected individually with modern electronics. The test chamber presented in this paper is not particularly optimized for CC but represents a typical chamber to be used in large scale experiments. The test setup presented here will not only be used to study the principles of CC but also related technological problems of a large realistic system. The apparatus was operated for the first time at the beam T9 of the CERN Proton Syncrotron (PS) in October 1995 in a short experiment to understand the behaviour of the setup and to measure the $\beta\gamma$ dependance of the CC mean. In this paper only the setup will be presented. The result of the CC will be the topic of a successive report.

1.0 THE CHAMBER

We built a drift chamber with 1 m long wires(fig.1) and with 147 square cells . A square cell 3x3 cm^2 (fig.2) has been chosen, because it is better adapted to detect particles randomly crossing the cell, like kaons decaying in flight far from the interaction point. A sense wire (30 µm golded tungsten) is surrounded by 12 field wires (100 µm copper beryllium). The chamber is filled with a mixture of 80% of He and 20% of CH_4 and operated in proportional regime. Particular care has been devoted to the gas tightness. We were able to obtain less than 50 ppm of oxygen with a flow of 5 l/min.The chamber has been operated at the lowest gain the electronic noise allowed, typically of the order of $1.5 \cdot 10^3$.

2.0 ELECTRONIC READOUT

In our setup the distribution of differences in arrival times of clusters is approximately an exponential with a mean value of the order of 40 ns. Details of the shape and mean values depend on the inpact parameter and cell orientation.
Most interesting in the analysis is the region of time differences of a few nanoseconds to study effects of diffusion and efficiency. The electronics has to have a time resolution better than the rise time of the fastest pulses and the desired separation.The signal has not to be integrated, but a 'picture' of its time development has to be taken with a time resolution of at least one ns. We designed and built a full electronic chain with analog bandwidth of 0.7 GHz and digitizer sampling frequency of 1 Gsamples per second.

2.1 PREAMPILFIER

Electronically the chamber has to be considered as a current source and the cell as a transmission line with an impedance of 470 Ohm. Both sides have to be terminated to avoid reflections simulating clusters. The preamplifier is designed(Fig.3) as a voltage amplifier based on the MAR6 from Mini-Circuits. The preamplifier has an input impedence of 470 Ohm, a gain of 10 per stage, 100 in total, and a BW limit of 0.7 GHz and it drives directly a 50 Ohm line. The main cut off in frequency comes from any lumped inductance like the legs of components for the signal pickup. Special care must then be devoted to the feedtrough to avoid a step in impedance and/or parasitic capacitance.The end cap of the chamber was covered by a printed circuit board with the high voltage decoupling capacitor and the first stage of the preamplifier directly at the feedtrough. The decoupling capacitor had 470 pF.The maximum cross talk we measured between the 72 PAs mounted is less than 2%. From the first stage the signal goes via 50 Ohm strips to the second stage at the edge of the board. A 50 Ohm high frequency coaxial cable is put to a SMA connector. The Input Equivalent Noise Charge of the pramplifiers results in about 350 electrons.
On the HV side the signal was adapted as well with an additional 100KOhms resistor toward the power supply.

2.2 DIGITIZERS

We developed the digitizers in a joint venture with Tektronix: the TVS 645, now available on the market . There are 4 channels per VXI module with these basic features:

- 1 GHz of analog BW
- 5 Gigasamples per second
- 8 bits vertical resolution (ENOB equal at 6.8 at 1 Gigasample per second; the module has been designed for a target resolution of 10 bits and uses 16 bits per word)
- a maximum of 32 Kbytes of buffer memory per event(waveform)
- a secondary memory of 96 kbytes to store events in AADV mode; the trigger rearming time is less than 200 ns.

The module can be read with a maximum of 1 Mwords per seconds.

We had 5 of these modules for a total of 20 channels. This allows (see fig.1) to get a maximum track lenght of 60 cm. We ran at 1 Gsamples per second for a maximum sampling time of 2 μs giving a total 4096 bytes per cell. One complete event consists of 80 Kbytes. The dynamic range of signal amplitude has been set between -40 and 10 mV.

2.3 NOISE

We measured the noise of the chamber plus amplifier plus cable using a scope with a band width of 1 GHz and a sampling frequency of 1 Gsamples per second. The rms of the digitized values is 0.8 mV. The same number determined with the digitizers gives 1.5 mV. A typical single electron signal has a FWHM of 10 nsec and a peak voltage of 6 mV. From these numbers one can roughly estimate a signal to noise ratio of about 16.

3.0 DATA ACQUISITION

We used a Macintosh Quadra 650 to read data and to store them on a DAT. The Nu-bus slots of the Macintosh have been equipped with a Micron card to access a Camac crate and with a National MXI-NB card to access the VXI crate. The full program for the data acquisition including device drivers has been written in C language.
The internal buffer of the TDS 645 was very usefull in managing the spill structure of the PS: one bunch of 400 msec each 14 sec. The overall acquisition rate we obtained was 10 events/spill.

4.0 BEAM SETUP AND TRIGGER

The beam setup is shown in Fig.4. For this test we needed an independent way to discriminate between particles speces at different beam momenta. In order to cover the $\beta\gamma$ region between 2 and 50, protons were selected for the lower $\beta\gamma$, kaons for the central region and pions for higher $\beta\gamma$ values. The properties of the beam have been well documented[6]. The most prominent features of the beam are a high abundance of pions for all settings and large suppression of kaons for positive charges. The startegy to get balanced number of particles was to use the available Tcherencov counter to reduce particles with high beta (almost all electrons and a momentum dependent fraction of pions). In next table the chosen beam momenta, trigger conditions and particle fractions in the collected data (R) are shown.

Beam mom.	trigger	π		K		P	
(Gev/c)		R(%)	$\beta\gamma$	R(%)	$\beta\gamma$	R(%)	$\beta\gamma$
1+	T*S1*/TC1	74	7.14			21	1.06
1.5+	T*S1*/TC1	78	10.7			18	1.6
2+	T*S1*/TC1	74	14.3			22	2.13
3-	T*S1*/TC1	46	21.4	34	6.1	20	3.2
4+	T*S1	65	28.6	5	8.1	23	4.2
4-	T*S1*/TC1	31	28.6	32	8.1	26	4.2
5-	T*S1*/TC1			76	10.1	18	5.3
5+	T*S1*/TC1					100	5.3

The trigger "T" was a coincidence between T1&T2 and T3&T4. T1,T2,T3 and T4 were four small 3x2 cm^2 and 5mm thick scintillator counters. They selected the track crossing the chamber. S1 is the first TOF counter and TC1 the Tcherencov.The chamber has been put at an angle of 45 degrees to the beam. For this test we did not plan to study the effects of the track angle.

4.1 TIME-OF-FLIGHT

To discriminate between residual π , K and (anti)protons we relied on the time-of-flight measurement between S1 and S3. S1 was a scintillator made of NE111, 3x6 cm^2 and 15 mm

thick. It had a light guide of 60 cm lenght to clear it from the magnet. S3 was a larger scintillator made of NE111, 15x15 cm^2 and also 15 mm thick. S1 was equipped with one and S3 with two (one per side) AVP56 photomultipliers. The signals S1, $S3_1$ and $S3_2$ were split to feed both a TDC and an ADC. The signal for the TDC was in turn split into two to feed different discriminators. The first one had a high thereshold for the trigger, while the second one had a thereshold of 10 mV. This last one was used to feed a TDC for the TOF measurement. The TDCs used were the LeCroy TDC 222 and set to a resolution of 100 psec per channel. Correcting all TDC values with the help of the ADC and averaging between $S3_1$ and $S3_2$ we obtained a resolution in TOF of 200 ps. This allows a separation of more than 3 sigmas between π and kaons at 4 GeV/c.
The fig.5 shows the TOF distribution of run 45, nominally at 3 GeV/c. We note the clear separation between particles types.

5.0 CONCLUSIONS AND DRIFT CHAMBER PERFORMANCES

Fig.6 shows a complete waveform for a typical hit, fig.7 shows typical peaks. In 4 days of main users time we collected about 60000 events with around 7000 events per momentum setting. A detailed description of the cluster counting algorithm and resolution obtained with this data will be presented in a forthcoming publication. If one uses only the arrival time of the first peak this chamber behaves like a normal drift chamber. To determine the T_0 two software corrections have been apported. As T_0 is used the extrapolation to the base line of the leading edge of the first peak. Further, the local average time spread is calculated from the average distance between the first 5 peaks and this value is used to correct the previously determined T_0 value. The drifttime-space-relation (fig.8) and the resolution as a funtion of the inpact parameter (fig.9) are determined. The resolution (lower than the expected one if one think that the He has a density 20 times lower than the Argon) and shows a flat behaviour at high IP. One can evaluate the cell width from T_0 and T_{last}. Fig. 9.1 shows the cell width determined in this way; its performs a resolution of 1.4%. Fig. 9.2 shows the track lenght calculated in this way versus the rack lenght resulting from the track reconstruction. Fig.10 shows a reconstructed track. With a cut on chi square at 0.5 mm and accepting events with at least 17 cells, we obtain a track reconstruction efficiency equal to 97.6 %. The same setup will be used for further studies.

ACKNOWLEDGEMENTS

We wish to thank the Coordinator and the full staff of the PS of the CERN for the perfect conditions and stability of the beam during our week of data taking. A big thanks goes to the A.Cattai team, Jean Martin and Christiane Bastie for their continous and crucial assistance during the setting up in site of the CERN.

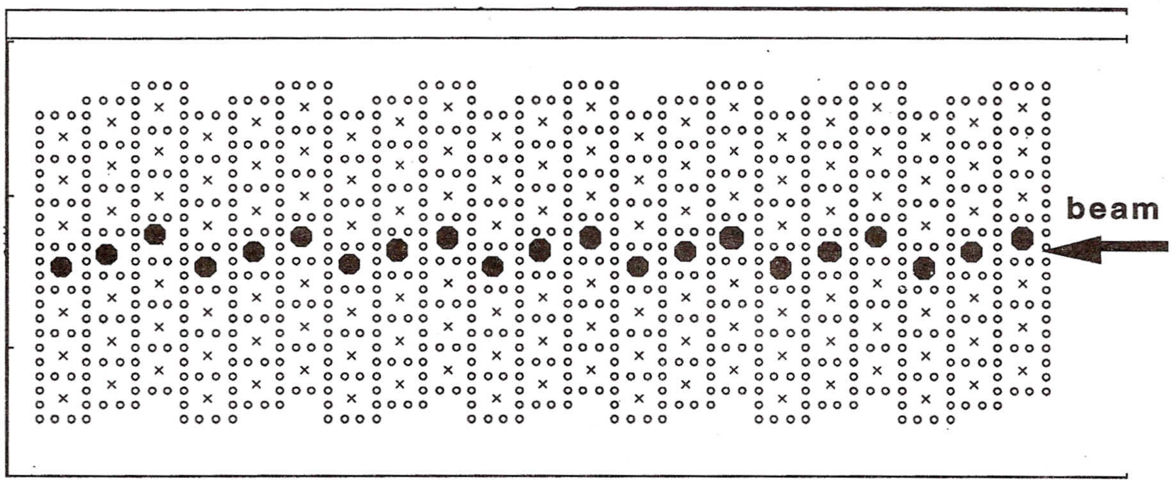

Figure 1 Cross section of the chamber. The dotted circles rapresents the sense wires equipped for cluster counting.

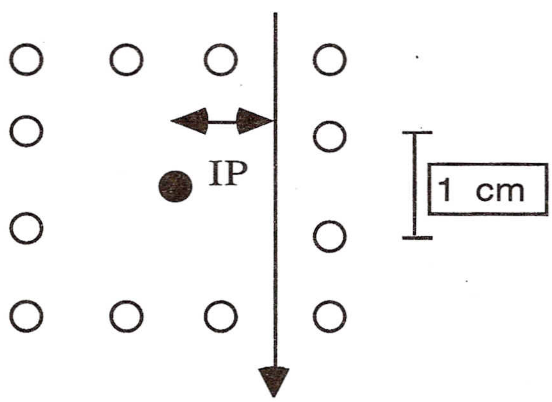

Figure 2 . Layout of the cell

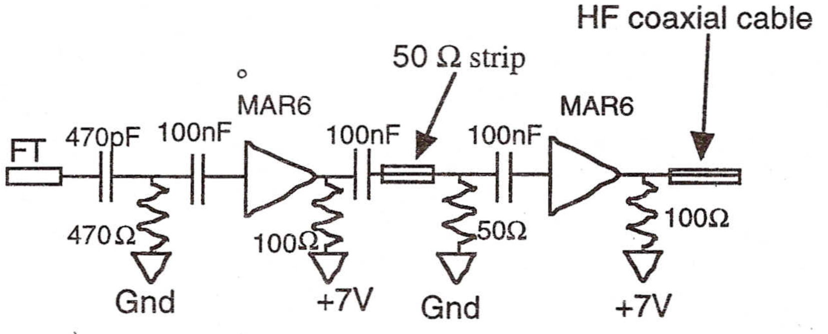

Signal pickup side

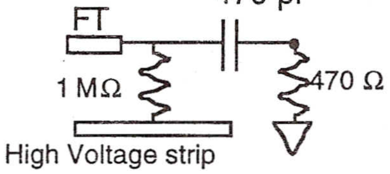

HV side

Figure 3 . Schematic diagram of the electronics for the pickup and the HV sides

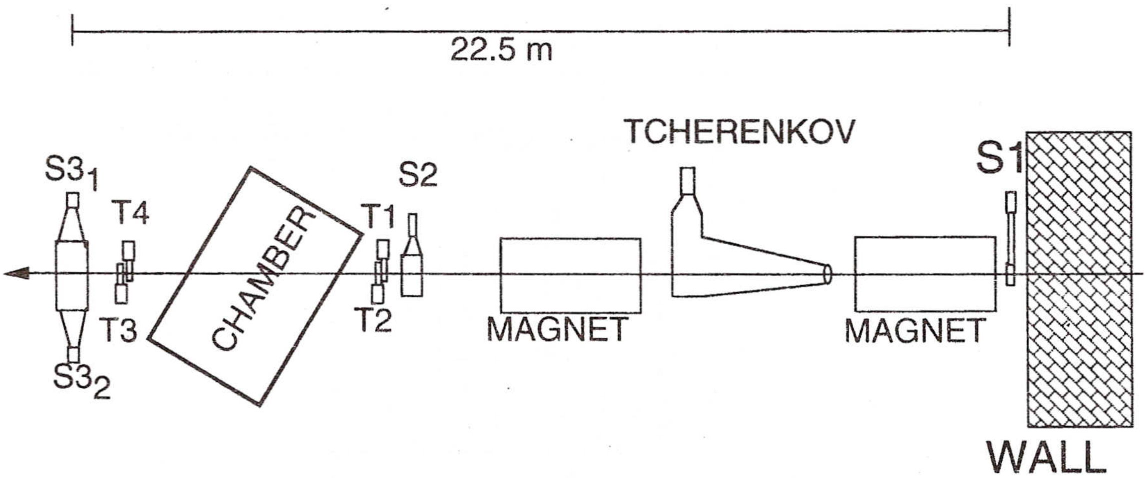

Fig.4
Beam Setup

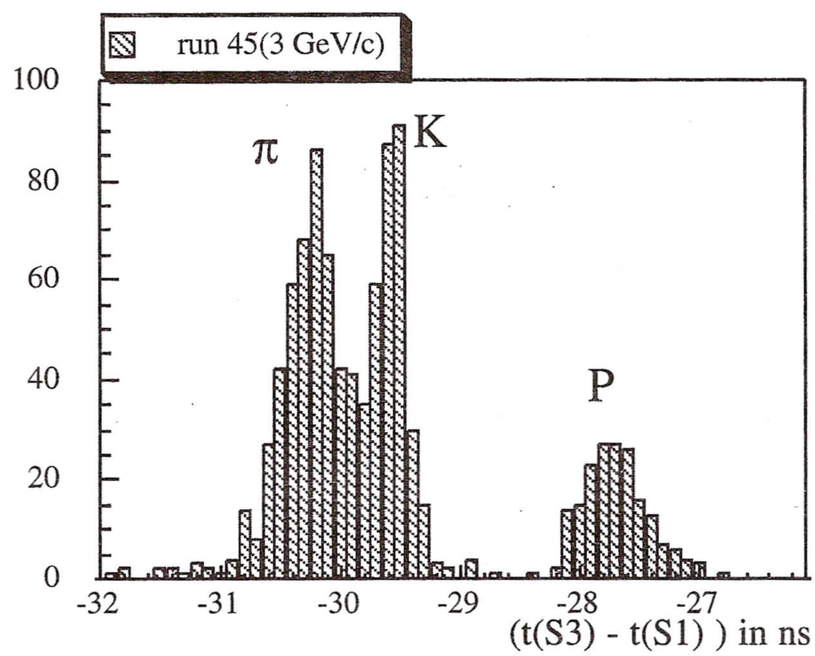

Figure 5 . TOF valus distribution for run 45 at 3 GeV/c. Values are ADC corrected and averaged between the two sides of S3.

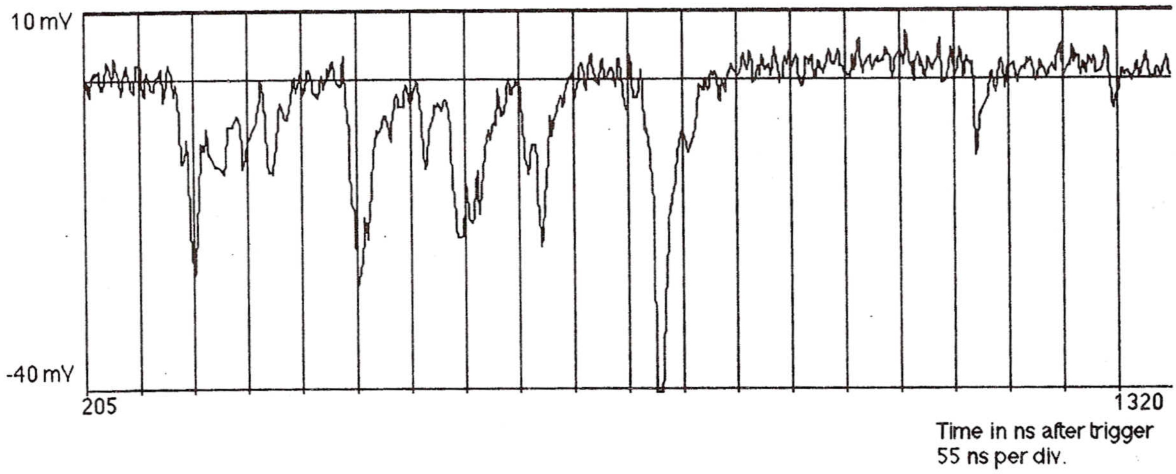

Figure 6 .A typical waveform shown in its relevant zone (205-1320 ns after trigger.

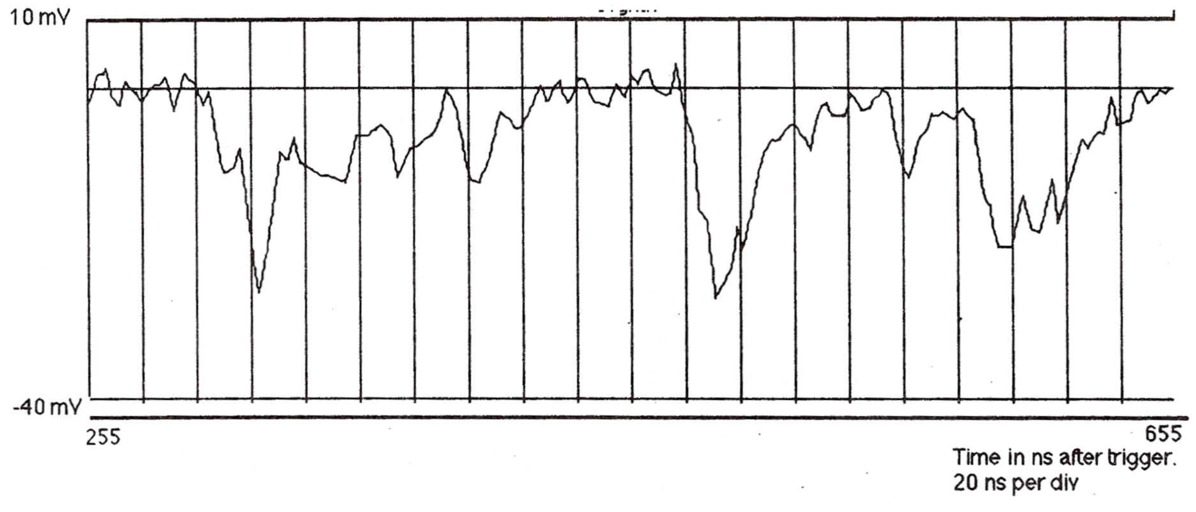

Figure 7 .The same wavêform as in fig.6 with a zoom on the first peaks.

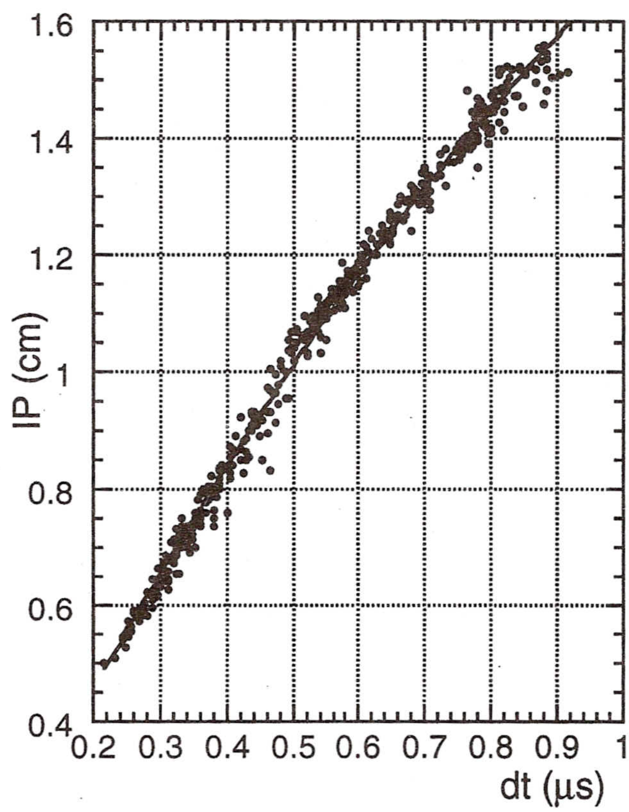

Figure 8 .The Inpact Parameter from the reconstructed track is plot vs the arrival time of the first cluster for wires not used in reconstructing the track.

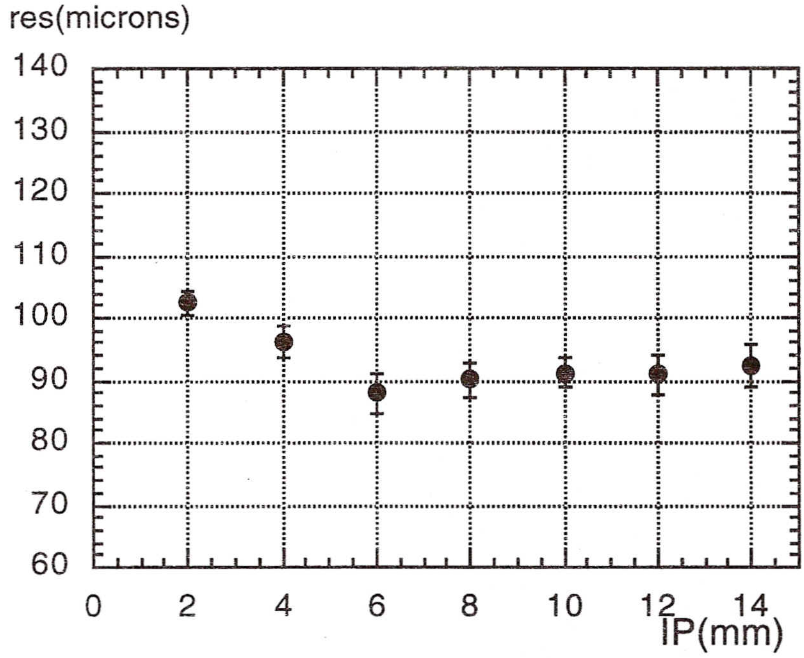

Figure 9 .Spatial resolution vs Inpact Parameter.

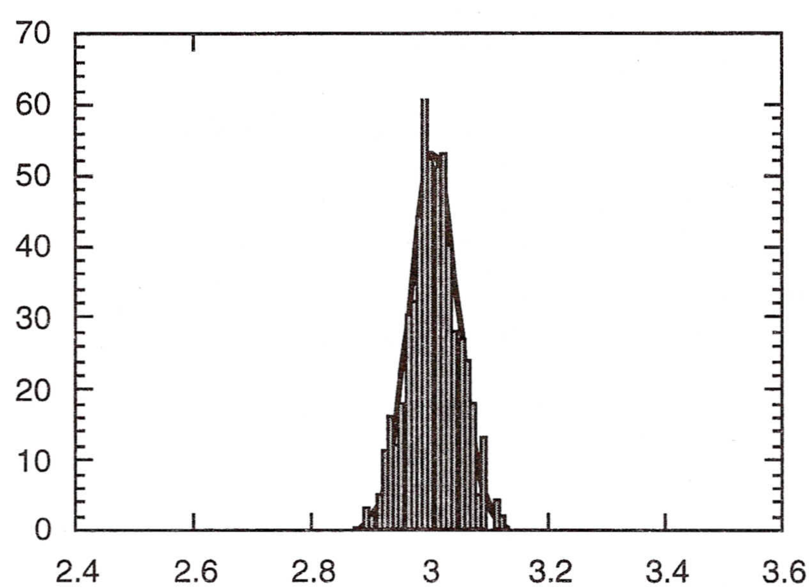

Figure 9.1 .Histogram of the cell width detrmined from the T_0 and T_{last}. The sigma is the 1.3% of the average value

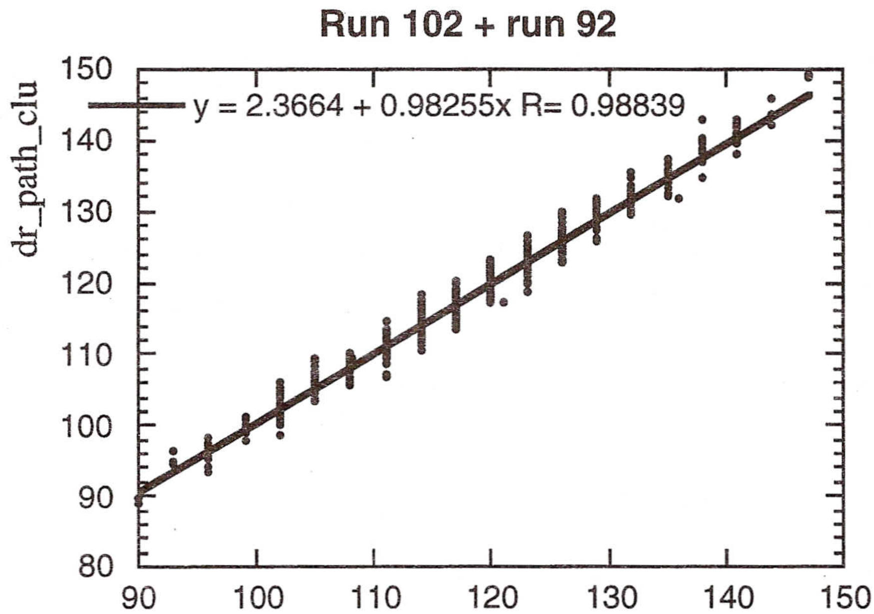

Figure 9.2 The track lenght calculated from T_0 and T_{last} is plotted vs the track lenght obtained form the track reconstruction.

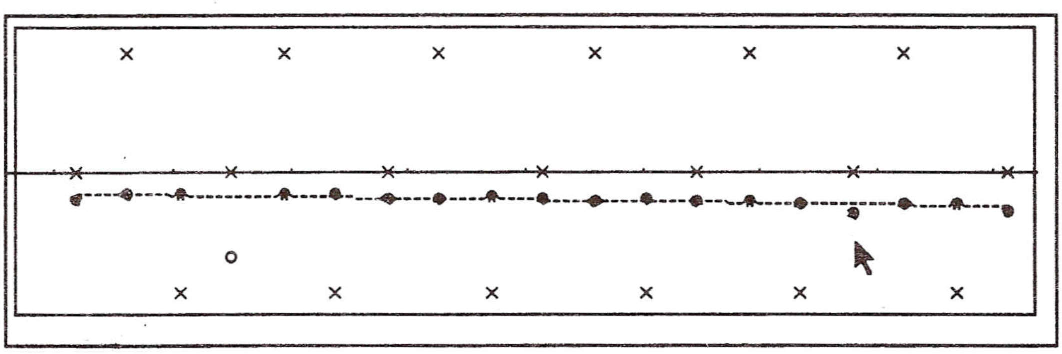

Figure 10 .The figure shows a track reconstructed. The "x" identifie the sense wires. The "•" the points deduced from the arrival time of the first signal and the dotted line the reconstructed track. Symbol "o" identifies signal discarded because out from the cut in chi square.

REFERENCES

1. Davidenko et al.
Measurement of the relativistic increase of the specific primary ionization in a streamer chamber.
NIM 67 (1969) 325-330

2. V.Eckardt et al
Particle Identification in a large streamer chamber with reduced memory time.
NIM 143 (1977) 235-239

3. A.H.Walenta
The Time expansion chamber and single ionization cluster measurement.
IEEE Transaction on Nuclear Science, Vol. NS-26,No.1, February 1979

4. P.Rehak and A.H.Walenta
Relativistic Rise measurement by cluster counting method in time expansion chamber
IEEE Transaction on Nuclear Science, Vol. NS-27, No.1, February 1980

5. A.Pansky et al.
Applications of gaseous electron counting detectors
Nuclear Instruments and Methods in Physics Research A323 (1992) 294-308

6. K.Batzner et al. , PS/PA - EP note 88-26, 8 august 1988